Eur. Phys. J. D **25**, 271–277 (2003)
DOI: 10.1140/epjd/e2003-00244-0

THE EUROPEAN PHYSICAL JOURNAL D

Three-dimensional effects in the modelling of ICPTs

Part I: Fluid dynamics and electromagnetics

D. Bernardi, V. Colombo[a], E. Ghedini, and A. Mentrelli

Dipartimento di Ingegneria delle Costruzioni Meccaniche, Nucleari, Aeronautiche e di Metallurgia (D.I.E.M.) and C.I.R.A.M., Università degli Studi di Bologna, Via Saragozza 8, 40123 Bologna, Italy

Received 22 May 2003
Published online 5 August 2003 –

Abstract. In this paper, we numerically investigate the 3-D effects of different flow operating conditions and of complete or simplified treatments of the electromagnetic field on the characteristics of Ar and Ar/N_2 discharges in inductively coupled plasma torches working at atmospheric pressure. Simulations are performed by means of the commercial code FLUENT© suitably customized to solve the electromagnetic field equations in the frame of an extended grid model. Steady state continuity, momentum and energy equations are solved for optically thin plasmas under the assumption of LTE and laminar flow. Results of parameterization on the net amount of power dissipated in the discharge, frequency of the RF generator, flow rate distribution of inlet gases and swirl velocity are presented, showing the impact of these parameters on the fluid dynamic and electromagnetic behaviour of the plasma.

PACS. 52.75.Hn Plasma torches – 52.65.-y Plasma simulation – 52.80.Pi High-frequency and RF discharges

1 Introduction

Modelling is a useful tool to investigate the characteristics of inductively coupled plasma torches, since an accurate characterization of the plasma discharge by means of typical diagnostic methods is very difficult to perform, especially for what concerns the flow field. Numerical modelling of this kind of devices involves the coupled solution of the fluid dynamic, energy and electromagnetic field equations for the plasma. The authors have recently developed a fully 3-D model [1–4] in the framework of the FLUENT© code to remove the axisymmetry assumption, which is the fundamental hypothesis of all the previous 2-D models [5–8], with the aim of predicting the non-axisymmetric effects induced by the actual shape of the induction coil. Apart from the increase in computational effort and in the number of governing scalar equations, the 3-D extension of the previous 2-D models implies that also the scalar potential must be taken into account, due to the presence of a space-varying electrical conductivity in the plasma discharge [9]. In this paper, we show the impact on the solution of using either a simplified or a complete electromagnetic model, taking into account or neglecting the scalar potential. Moreover, a parameterization on the net amount of power dissipated in the discharge and on the working frequency of the RF generator is performed. Investigations on the plasma fluid dynamics are carried out for different distributions of inlet gas flow rates and swirl velocity magnitude and direction, in order to highlight the effects of such parameters on the 3-D behaviour of the discharge. Finally, a comparison of results obtained using pure argon and Ar/N_2 mixture as plasma gas is performed.

In the second part of this work [3], the attention will be focused on the impact of different coil shapes and torch geometries on the characteristics of pure argon discharges. Simulation results will be presented for conventional helicoidal, planar and double-stage coil configurations and for a torch with elliptical cross-section. Moreover, the effects of reducing the post-coil length on plasma temperature and velocity distributions will be shown for the same torch geometry considered in this paper.

2 Torch geometry and mathematical model

Torch geometry (referring to Tekna Plasma Systems Inc., PL-50 model) and common operating conditions employed in the following simulations are shown in Figure 1. Corresponding dimensions are summarized in Table 1. The complete electromagnetic field approach includes the 3-D governing equations for the vector potential,

[a] e-mail: colombo@ciram.ing.unibo.it

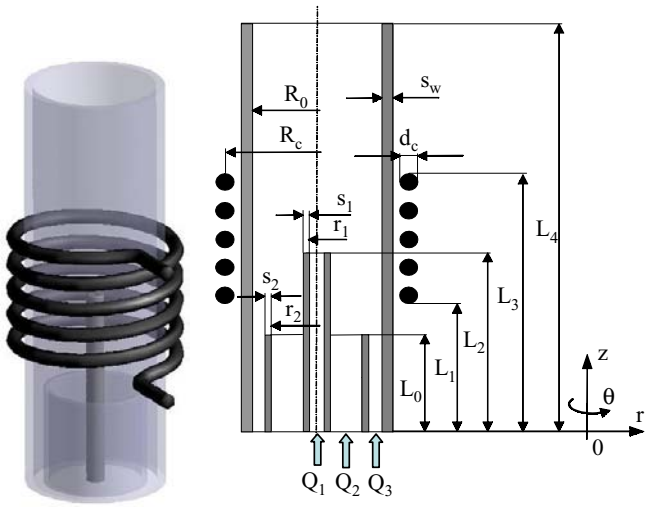

Fig. 1. (a) 3-D schematic reproducing the actual coil and (b) dimensions of the plasma torch.

Table 1. Dimensions and operating conditions.

$r_1 = 1.7$ mm	$R_0 = 25$ mm
$r_2 = 18.8$ mm	$R_c = 33$ mm
$s_1 = 2$ mm	$d_c = 6$ mm
$s_2 = 2.2$ mm	$s_w = 3.5$ mm
$L_0 = 40$ mm	$L_3 = 110$ mm
$L_1 = 50$ mm	$L_4 = 170$ mm
$L_2 = 80$ mm	
Pressure $= 1.013 \times 10^5$ Pa	

$\mathbf{A} = (A_x, A_y, A_z)$, and for the scalar potential, V:

$$\boldsymbol{\nabla}^2\mathbf{A} - \mu_0\sigma(\boldsymbol{\nabla}V + \partial\mathbf{A}/\partial t) + \mu_0\mathbf{J}^{\text{coil}} = 0, \quad (1)$$

$$\boldsymbol{\nabla}\cdot[\sigma(\boldsymbol{\nabla}V + \partial\mathbf{A}/\partial t)] = 0. \quad (2)$$

Here, μ_0 is the magnetic permeability of the free space, σ is the plasma electric conductivity and $\mathbf{J}^{\text{coil}} = (J_x^{\text{coil}}, J_y^{\text{coil}}, J_z^{\text{coil}})$ represents the current density in the coil region, which is calculated as: $\mathbf{J}^{\text{coil}} = (I/S_c)\mathbf{j}_{\text{coil}}$, where I is the total electric current flowing through the coil, $\mathbf{j}_{\text{coil}}$ is a unit vector perpendicular to the cross-sections of each coil turn and S_c is the area of these cross-sections. Displacement current associated with the oscillatory magnetic field has been assumed negligible. The electric ($\mathbf{E}$) and magnetic ($\mathbf{B}$) fields can be expressed through the definitions of the vector and scalar potentials as: $\mathbf{E} = -\partial\mathbf{A}/\partial t - \boldsymbol{\nabla}V$, $\mathbf{B} = \boldsymbol{\nabla}\times\mathbf{A}$. The simplified electromagnetic model is obtained neglecting equation (2) that takes into account the electric charge distribution arising in the discharge due to the space-varying conductivity of the plasma. Vanishing boundary conditions and a computational mesh extending outside the plasma region [6,7] are adopted within the UDS technique [8] for the FLUENT©-based solution of equations (1, 2), as done in [1]. Three-dimensional continuity, Navier-Stokes and energy equations are solved together with the electromagnetic ones for optically thin plasmas under the assumptions of local thermodynamic equilibrium and laminar flow.

3 Selected results

Where not specified, the results presented here refer to two perpendicular planes passing through the axis of the torch, whose relative position is evidenced by coil view. In the following, P denotes the net amount of power dissipated in the discharge, f is the frequency of the RF generator, while Q_1, Q_2, Q_3 are the carrier, plasma and sheath gas flow rates, respectively. For each case, detailed operating conditions are summarized in the corresponding figure caption. Plasma temperature and velocity fields calculated within the framework of the simplified electromagnetic model for an argon operated torch with net power dissipated in the discharge $P = 25$ kW and without inlet gas swirl velocity are shown in Figure 2, in order to introduce a reference case to which compare the other results. In particular, Figures 2a and 2c show a strong non axisymmetry of the discharge and a maximum of the plasma temperature located near the quartz confinement tube. The effects of using the complete electromagnetic model are shown in Figure 3, for the same operating conditions of the previous case. Plasma temperature differences between the two cases are negligible, while the tangential velocity obtained using the complete model reduces its magnitude with respect to that calculated with the simplified one. Real and imaginary components of the electric charge density distribution that arises because of the plasma conductivity gradient is shown in Figure 4. Electric charges are mainly located in the regions where the maximum values of the gas temperature gradient occur. Corresponding scalar potential fields, whose source is the charge density, are shown in Figure 5. Temperature fields obtained introducing a swirl velocity component $v_{\theta s} = \pm 20$ m/s in the sheath gas, are presented in Figure 6, showing that the presence of such component induces a better confinement of the plasma discharge with respect to the previous cases, and that the maximum temperature zone is far from the quartz tube, avoiding the risk of its melting. Figure 6 puts also into evidence that a change in the swirl direction of the sheath gas leads to much different results in the temperature fields at the torch exit and in the upstream region of the discharge, as a consequence of the complex 3-D fluid dynamic phenomena that occur in the torch. As an alternative to the previous case, a swirl component $v_{\theta p} = \pm 20$ m/s is applied to the plasma gas; corresponding results are reported in Figure 7, showing a lower efficiency in the discharge confinement with respect to the case with swirl velocity component in the sheath gas. Reducing the power dissipated in the discharge to a value of 15 kW, with a swirl component in the sheath gas $v_{\theta s} = +10$ m/s, leads to the results of Figures 8 and 9, corresponding, respectively, to the cases with and without carrier gas. The effects of an increase in the RF generator frequency from

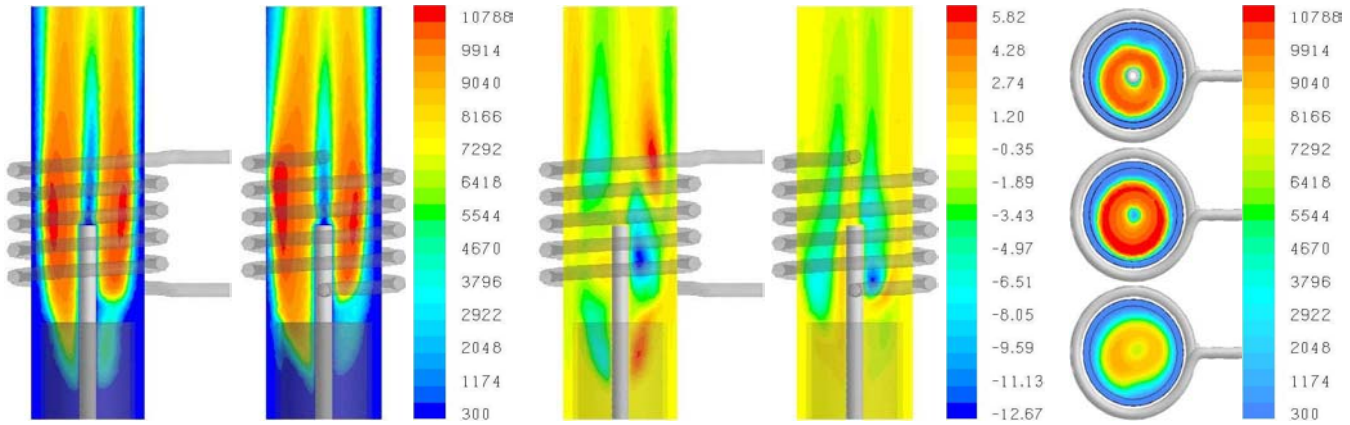

Fig. 2. $P = 25$ kW; $f = 3$ MHz; $Q_1/Q_2/Q_3 = 10/30/120$ slpm; working gas: Ar; (a) plasma temperature [K] and (b) tangential velocity [m/s] fields, calculated using the simplified e.m. model; (c) plasma and wall temperature fields [K] on three horizontal planes located at $z = 60$, 90, 170 mm respectively, from top to bottom. Color figures are available at `http://www.edpsciences.org/epjd/`.

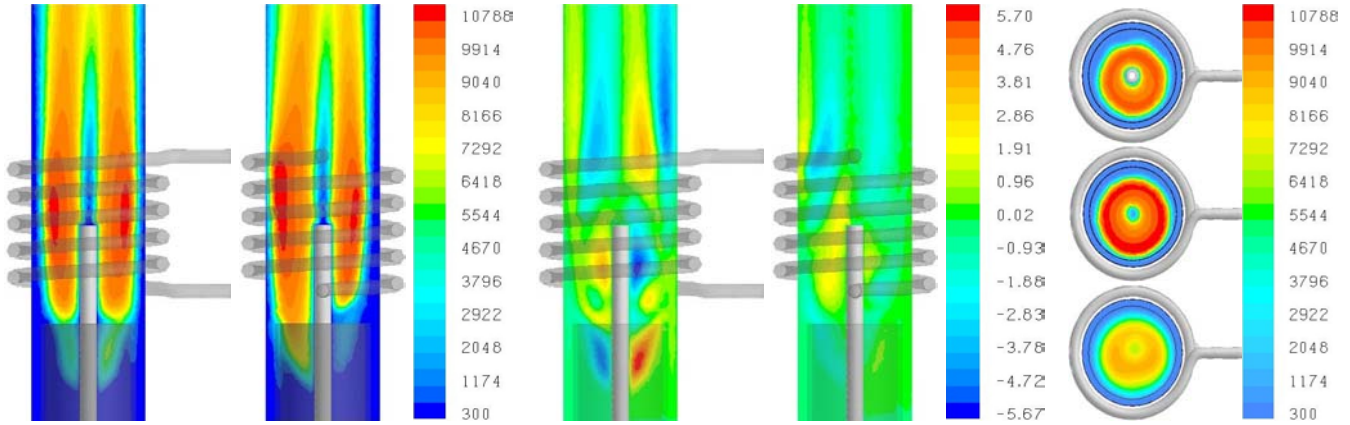

Fig. 3. $P = 25$ kW; $f = 3$ MHz; $Q_1/Q_2/Q_3 = 10/30/120$ slpm; working gas: Ar; (a) plasma temperature [K] and (b) tangential velocity [m/s] fields, calculated using the complete e.m. model; (c) plasma and wall temperature fields [K] on three horizontal planes located at $z = 60$, 90, 170 mm respectively, from top to bottom.

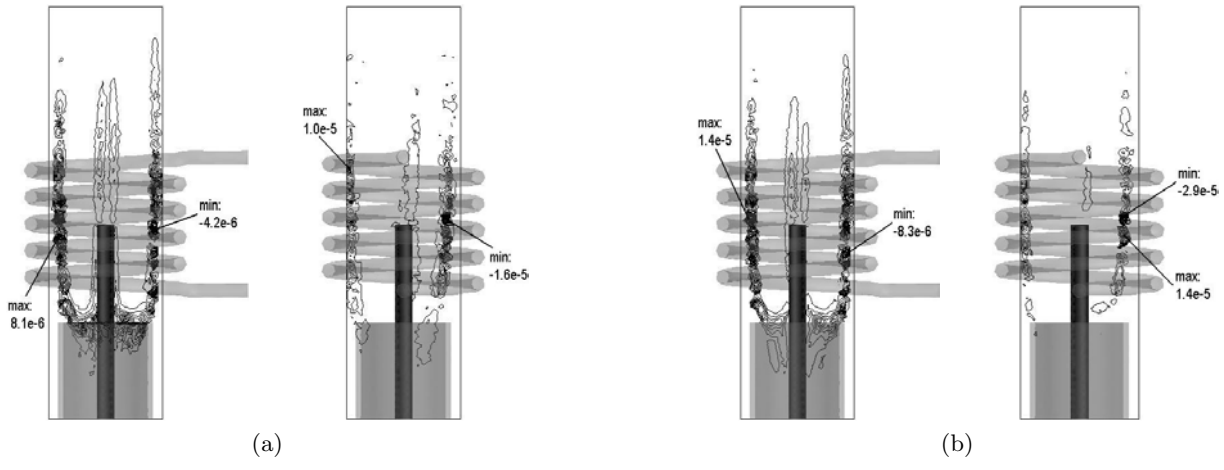

Fig. 4. (a) Real and (b) imaginary parts of the electric charge density distribution [C/m^3] in the plasma, for the case of Figure 3.

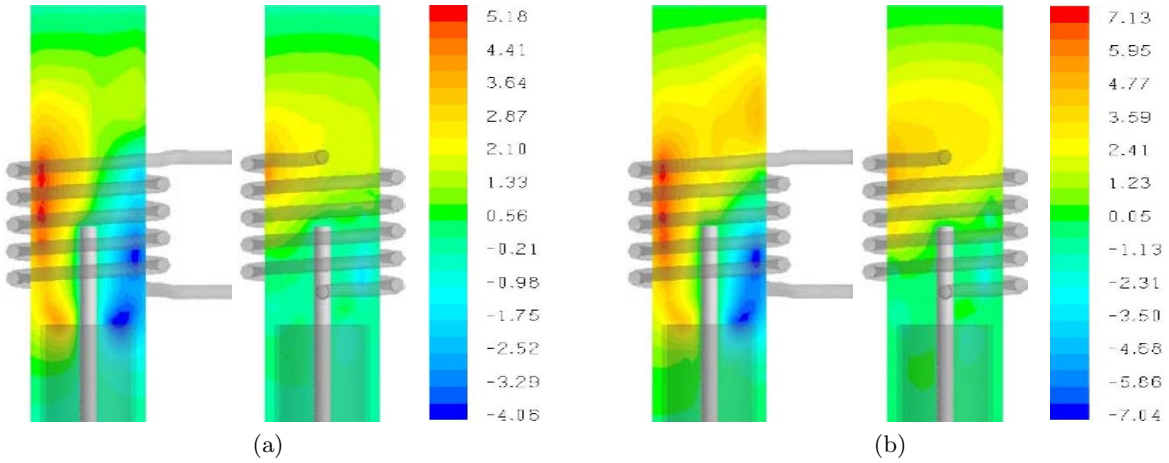

Fig. 5. (a) Real and (b) imaginary parts of the scalar potential field [V] in the plasma, for the case of Figure 3.

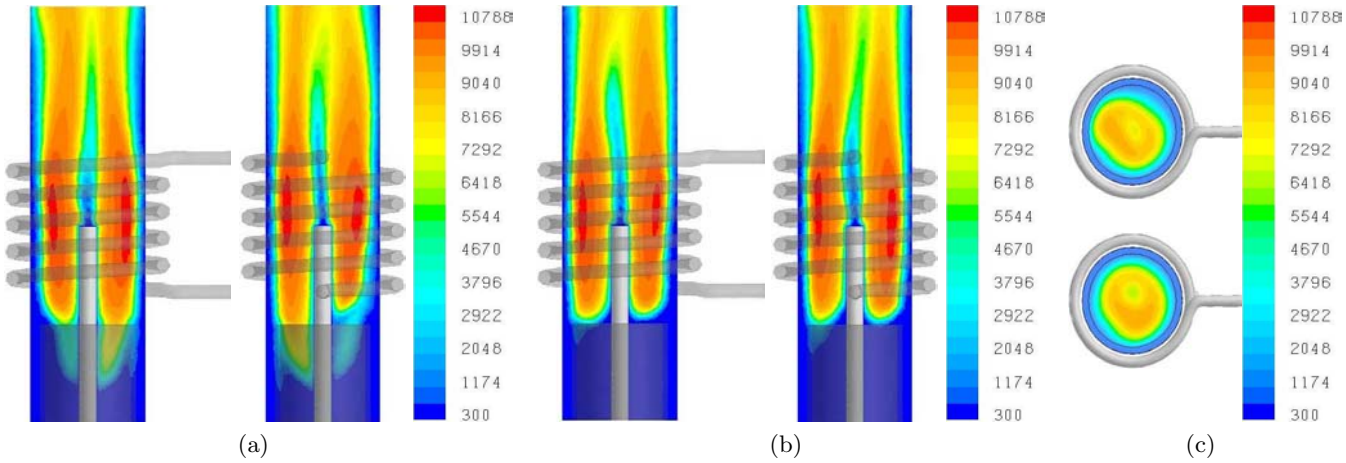

Fig. 6. (a) Plasma temperature [K] fields, calculated using the simplified e.m. model, for the same case of Figure 2 but with $v_{\theta s} = 20$ m/s; (b) as in (a) but with $v_{\theta s} = -20$ m/s; (c) plasma and wall temperature fields [K] at the torch exit for the cases (a) and (b) respectively, from top to bottom.

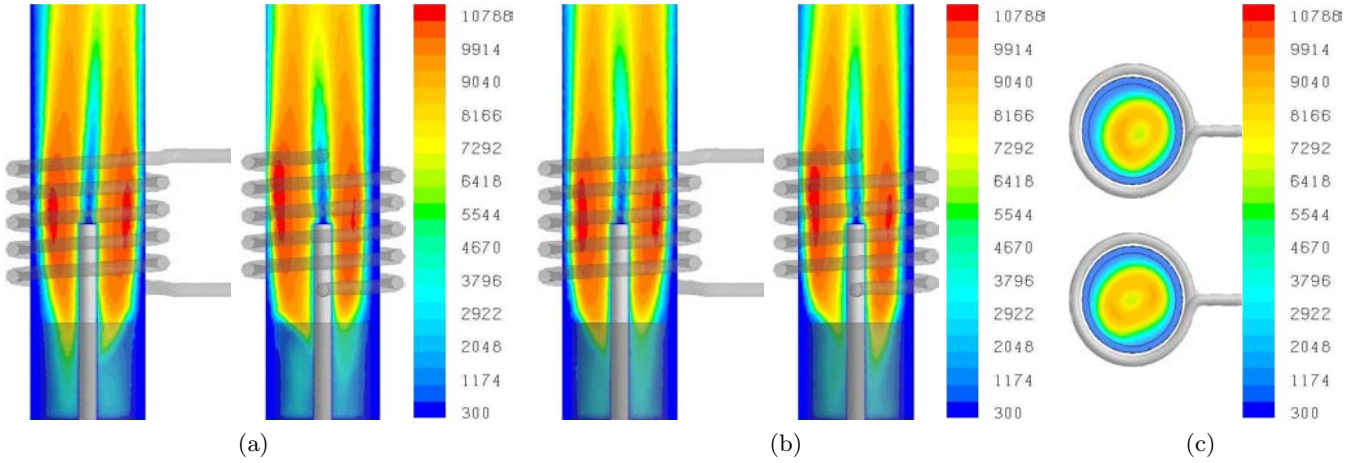

Fig. 7. (a) Plasma temperature fields [K], calculated using the simplified e.m. model, for the same case of Figure 2 but with $v_{\theta p} = 20$ m/s; (b) as in (a) but with $v_{\theta p} = -20$ m/s; (c) plasma and wall temperature fields [K] at the torch exit for the cases (a) and (b) respectively, from top to bottom.

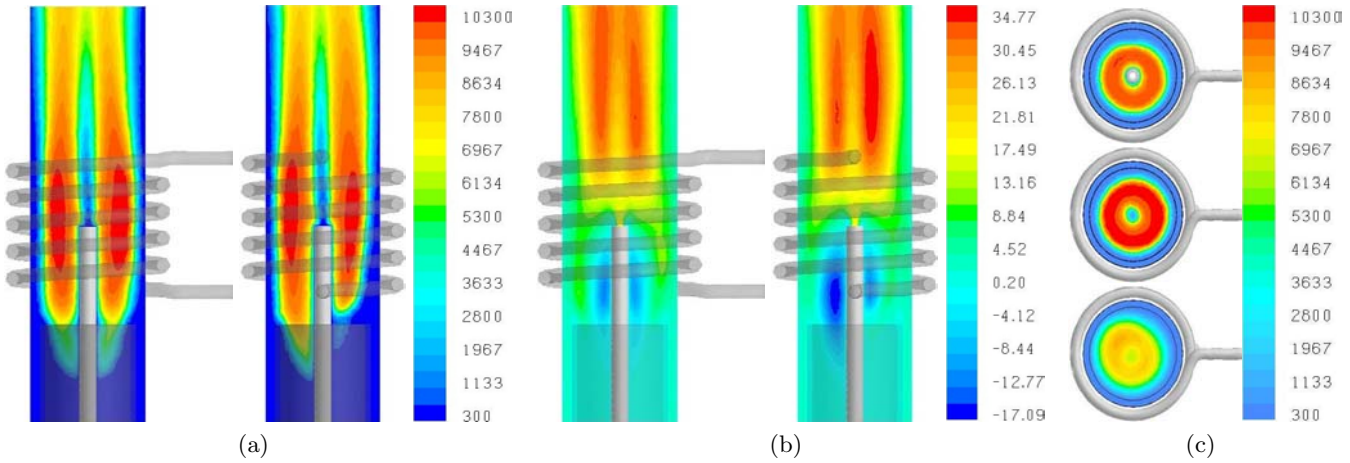

Fig. 8. $P = 15$ kW; $f = 3$ MHz; $Q_1/Q_2/Q_3 = 10/30/120$ slpm; $v_{\theta s} = 10$ m/s; working gas: Ar; (a) plasma temperature [K] and (b) axial velocity fields [m/s], calculated using the simplified e.m. model; (c) plasma and wall temperature fields [K] on three horizontal planes located at $z = 60$, 90, 170 mm respectively, from top to bottom.

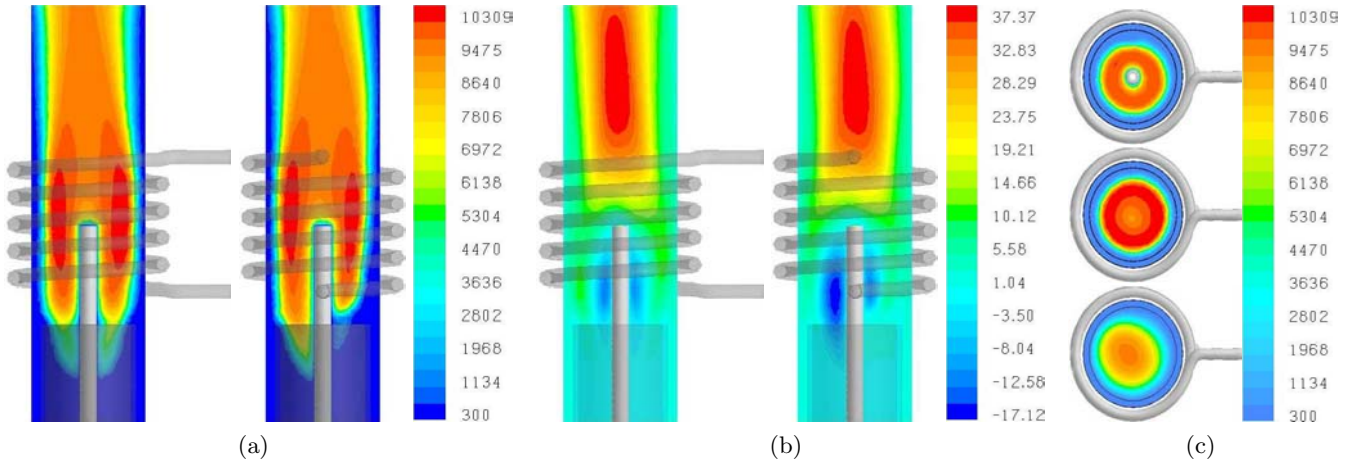

Fig. 9. $P = 15$ kW; $f = 3$ MHz; $Q_1/Q_2/Q_3 = 0/30/120$ slpm; $v_{\theta s} = 10$ m/s; working gas: Ar; (a) plasma temperature [K] and (b) axial velocity fields [m/s], calculated using the simplified e.m. model; (c) plasma and wall temperature fields [K] on three horizontal planes located at $z = 60$, 90, 170 mm respectively, from top to bottom.

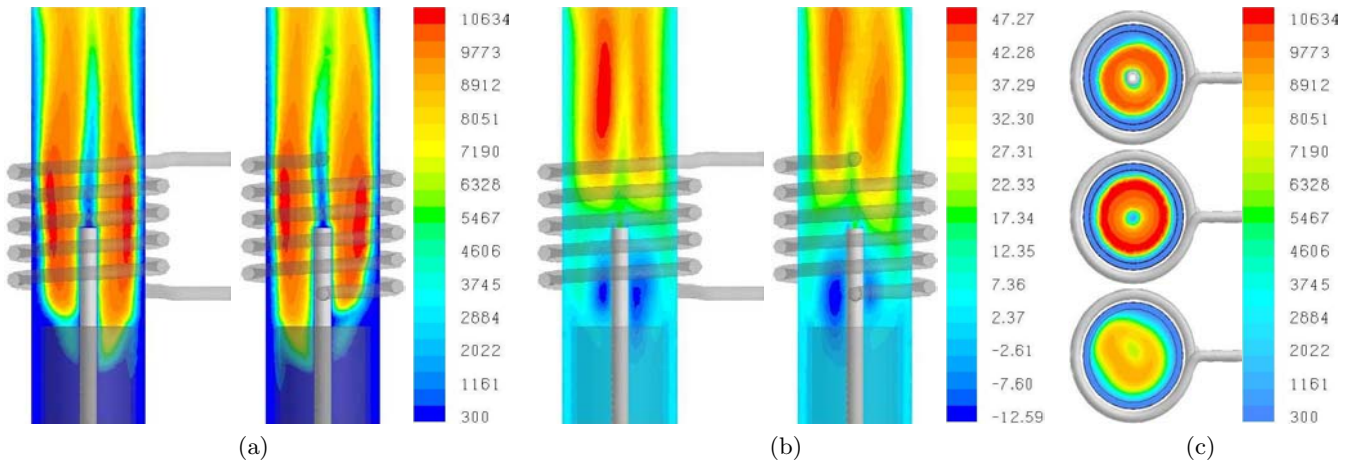

Fig. 10. $P = 25$ kW; $f = 5$ MHz; $Q_1/Q_2/Q_3 = 10/30/120$ slpm; $v_{\theta s} = 20$ m/s; working gas: Ar; (a) plasma temperature [K] and (b) axial velocity fields [m/s], calculated using the simplified e.m. model; (c) plasma and wall temperature fields [K] on three horizontal planes located at $z = 60$, 90, 170 mm respectively, from top to bottom.

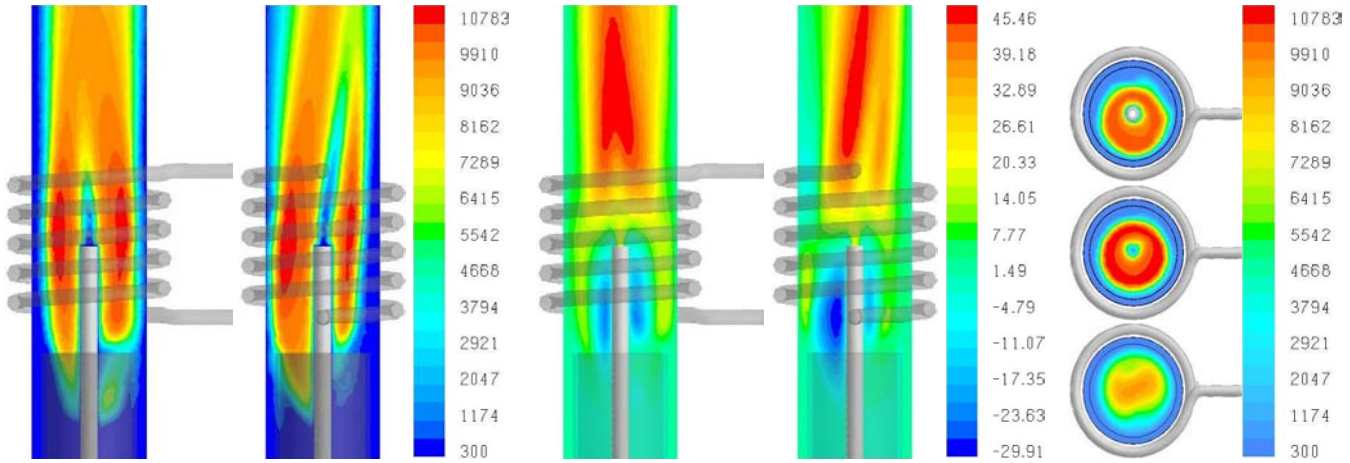

Fig. 11. $P = 25$ kW; $f = 3$ MHz; $Q_1/Q_2/Q_3 = 10/30/120$ slpm; $v_{\theta s} = 0$; $v_{\theta p} = 0$; working gas: Ar/N_2 (5% by volume); (a) plasma temperature [K] and (b) axial velocity fields [m/s], calculated using the simplified e.m. model; (c) plasma and wall temperature fields [K] on three horizontal planes located at $z = 60$, 90, 170 mm respectively, from top to bottom.

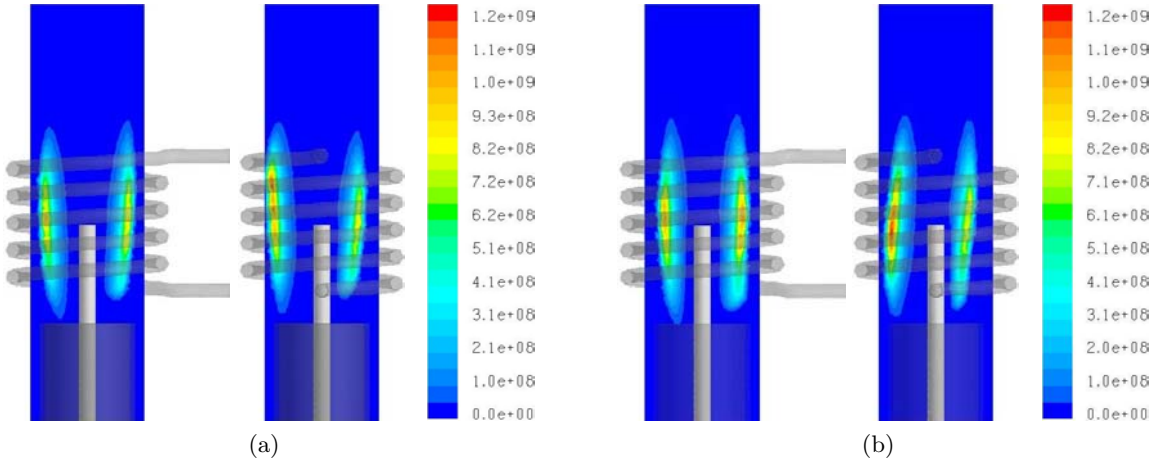

Fig. 12. Power density distributions [W/m^3] for the cases corresponding to (a) Figure 2 (working gas: Ar) and (b) Figure 11 (working gas: Ar/ N_2, 5% by volume).

3 MHz to 5 MHz are shown in Figure 10. Finally, Figures 11 and 12 show the impact of using Ar/N_2 (5% by volume) instead of pure argon on the plasma temperature and velocity fields and on the power density distribution.

4 Conclusions

Investigations performed in this work show that 3-D effects in inductively coupled plasma torches play an important role in the physical characterization of the discharge. As a first approximation, the electromagnetic equations can be solved neglecting the scalar potential to obtain quite accurate results for the plasma temperature. Anyway, the authors suggest that a complete electromagnetic model should be used if a detailed prediction of the plasma fluid dynamics in the discharge is desired, even though the consistency between this model and its numerical treatment implying the arising of results that show the existence of an electric charge density distribution in the plasma need to be further investigated in the frame of a supposedly requested fulfillment of the quasi-neutrality condition. The complexity of the phenomena involved in this kind of devices, especially for what concerns the fluid dynamics, let the results be quite difficult to foresee when changing the torch operating parameters. For this reason, the 3-D code developed by the authors can be a useful tool in the design of inductively coupled plasma torches. Also important as a next step in this research will be the comparisons between numerical and experimental results under different torch operating conditions and geometries, in order to test and tune the code [4].

The authors would like to thank Leonardo Seccia and Riccardo Rossi for the use of the parallel calculation facilities at CTFD-Lab of the Faculty of Engineering in Forlì, Italy. This

work was performed with partial financial support from the University of Bologna Goal-Oriented project 2001-2003 and ex-60% 2001-2002 projects, from the Italian Ministry of Education, University and Scientific Research (M.I.U.R.) national project COFIN2002.

References

1. D. Bernardi, V. Colombo, E. Ghedini, A. Mentrelli, Eur. Phys. J. D **22**, 119 (2003)
2. D. Bernardi, V. Colombo, E. Ghedini, A. Mentrelli, Three-Dimensional Modelling of Inductively Coupled Plasma Torches, *16th International Symposium on Plasma Chemistry*, Taormina, Italia, 22-28 June 2003
3. D. Bernardi, V. Colombo, E. Ghedini, A. Mentrelli, Eur. Phys. J. D **25**, 279 (2003)
4. V. Colombo, G. Gao, E. Ghedini, J. Mostaghimi, Asymmetry Effects in the Diagnostics and Simulation of RF Inductively Coupled Plasma Torch, *16th International Symposium on Plasma Chemistry*, Taormina, Italia, 22-28 June 2003
5. J. Mostaghimi, M.I. Boulos, Plasma Chem. Plasma Process. **9**, 1 (1988)
6. V. Colombo, C. Panciatichi, A. Zazo, G. Cocito, L. Cognolato, IEEE Trans. Plasma Sci. **25**, 5 (1997)
7. S. Xue, P. Proulx, M.I. Boulos, J. Phys. D: Appl. Phys. **34**, 1897 (2001)
8. D. Bernardi, V. Colombo, E. Ghedini, A. Mentrelli, Eur. Phys. J. D, e-print `DOI: 10.1140/epjd/e2003-00227-1` (2003)
9. D. Bernardi, V. Colombo, E. Ghedini, A. Mentrelli, Three-Dimensional Effects in the Design of Inductively Coupled Plasma Torches, *XVI Congresso Nazionale Sulla Scienza e Tecnologia del Vuoto*, Catania, Italia, 7-9 October 2002